

## Non-Shock Initiation Model for Explosive Families: Experimental Results

Mark U. Anderson\*, Steven N. Todd\*, Terry L. Caipen<sup>f</sup>, Charles B. Jensen\*, and Chance G. Hughs<sup>x</sup>

\*Sandia National Laboratories, Albuquerque, NM, 87185

<sup>f</sup>Applied Research Associates, Albuquerque, NM, 87110

<sup>x</sup>North Vector, Menlo Park, CA, 94025

**Abstract.** The “DaMaGe-Initiated-Reaction” (DMGIR) computational model has been developed to predict the response of ideal high explosives to impulsive loading from non-shock mechanical insults. The distinguishing feature of this model is the introduction of a damage variable, which relates the evolution of damage to the initiation of a reaction in the explosive, and its growth to detonation. This model development effort treats the non-shock initiation behavior of explosives by families; rigid plastic bonded, cast, and moldable plastic explosives. Specifically designed experiments were used to study the initiation process of each explosive family with embedded shock sensors and optical diagnostics. The experimental portion of this model development began with a study of PBXN-5 to develop DMGIR model coefficients for the rigid plastic bonded family, followed by studies of the cast, and bulk-moldable explosive families, including the thermal effects on initiation for the cast explosive family. The experimental results show an initiation mechanism that is related to impulsive energy input and material damage, with well defined initiation thresholds for each explosive family. These initiation details will be used to extend the predictive capability of the DMGIR model from the rigid family into the cast and bulk-moldable families.

---

### Introduction

The impulsive load caused by the impact of a projectile or fragment into an energetic material will produce a range of responses that can range from mechanical damage with no reaction to a self-sustaining deflagration that consumes the material at an increasing rate, transitioning into a detonation.

The magnitude of impulsive energy input, and the extent to which damage is generated in the energetic material have a direct effect on the onset

and the extent of reaction produced in an explosive sample. Impact-induced deflagrations with sufficient energy input and mechanical damage have been observed to transition within a few microseconds into a growth to detonation. The generation of damage is dependent on the shock loading and unloading profile, and the material strength. Numerical simulations of this damage are used to relate shear-induced strain to explosive initiation by the use of a damage variable which is embedded in the DMGIR non-shock initiation model. This treatment of non-shock initiation

allows all ideal explosives to be described numerically in one of the following three explosive families; rigid plastic bonded, cast, and moldable plastic explosives.<sup>1</sup>

An experimental program was designed which made use of embedded shock sensors and optical diagnostics in order to better understand the explosive initiation process of these explosive families from impulsive, non-shock loading.

## Experimental Description

A single-stage light gas, or a propellant gun was used in each test to accelerate a projectile to the desired velocity, impacting an explosive test specimen. Projectile free flight of ~8-feet allowed blast protection for the gun. The test specimen was either a solid or a sandwiched cylindrical billet, instrumented with PVDF piezoelectric shock sensors for velocity measurements.<sup>2</sup> Digital framing cameras recorded the details of projectile impact and subsequent reaction on each experiment. Thermal effects on the cast explosive family were evaluated at temperatures that ranged from ambient to 122C. The ambient temperature test configuration is shown schematically in Fig. 1.

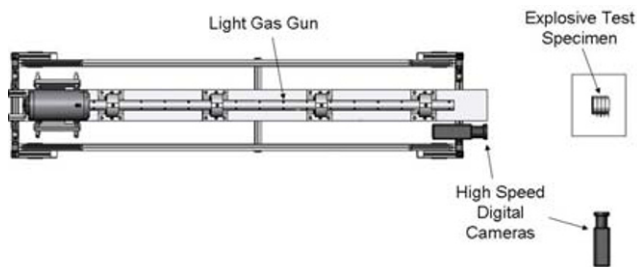


Fig. 1. Gun configuration for explosive study.

The projectile geometry consisted of a blunt-faced, hollow, right circular cylinder with a 0.500-inch diameter and an O-ring groove near the impact face. Projectile materials were aluminum or brass.

This projectile design provided a planar, short duration shock loading pulse, followed immediately by axial and radial rarefaction waves which provide well controlled mechanical damage, as shown in Fig. 2. This controlled damage was intended to simulate the expected profile produced by accidental impact.<sup>3</sup> Impact velocity capabilities

range from 0.20 – 1.66 km/s. Explosively driven water blades were also used to generate mechanical damage, although less well controlled.

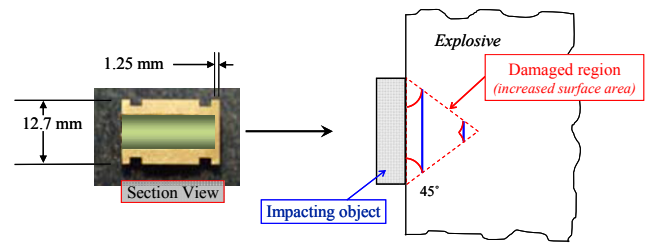


Fig. 2. Shock and release from projectile impact generates a controlled damage region in explosive.

## Test Specimen

Ideal explosives are composite materials with explosive crystals embedded in a variety of polymer-based binders, with mechanical properties that depend mainly on the mixture used to form the polymer binder. The three explosive families described in this study were represented by: PBXN-5,  $\rho=1.80$  gm/cc, (rigid plastic bonded), cast Composition-B,  $\rho=1.61$  and  $1.67$  gm/cc, (cast), and PETN- or RDX-based Primasheet 1000, 2000, and Composition C-4,  $\rho=1.60$  gm/cc (moldable plastic).

The ambient temperature test specimen configurations consisted of a cylindrical billet that was made from sandwiched billets with piezoelectric shock sensors embedded at each interface. Billet diameters were nominally 4.0-inch diameter. The piezoelectric shock sensors measured stress-time history along the axial centerline of the PBXN-5 billet. Shock front arrival times for each sensor location are plotted in Fig. 3 for a collection of PBXN-5 tests, showing the transition region between the mechanical response and the deflagration growth to detonation, as well as prompt detonation response from detonator input.

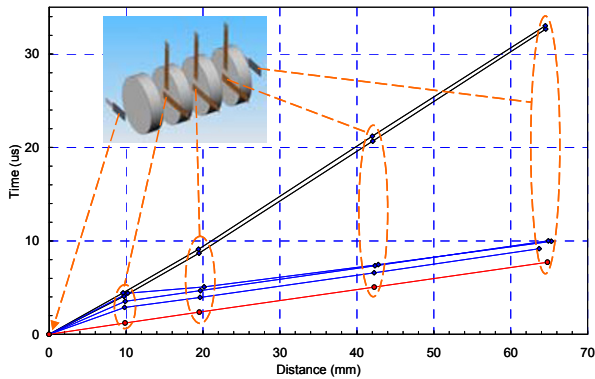


Fig. 3. Instrumented test sample of PBXN-5 with embedded piezoelectric shock sensors. Shock arrival data is plotted for multiple PBXN-5 tests.

The embedded Bauer PVDF shock sensor thickness was 25  $\mu\text{m}$ , insulated on both sides with 50  $\mu\text{m}$  Teflon<sup>TM</sup>. MSI Piezofilm<sup>TM</sup> sensors were used on front and rear surfaces for timing measurements, augmenting the embedded shock sensor measurements on the sandwiched billets. The impact surface Piezofilm<sup>TM</sup> sensor also provided the instrumentation trigger signal.

### Shock Propagation Results

The piezoelectric output from each shock sensor provides a wave propagation measurement with a timing uncertainty of  $\pm 4$  ns, based on the 2 ns sampling interval. Average velocity between each shock sensor location is based on thickness measurements along the billet centerline and transit time between sensor locations. Shock propagation time through each sensor package is removed prior to velocity calculations. Prompt-detonation control experiments were conducted to measure material response for each family under Shock-to-Detonation Transition (SDT) conditions. The PBXN-5 data set from Fig. 3 is plotted in velocity-vs-distance space in Fig. 4 to illustrate the observed non-shock initiation behavior for PBXN-5.

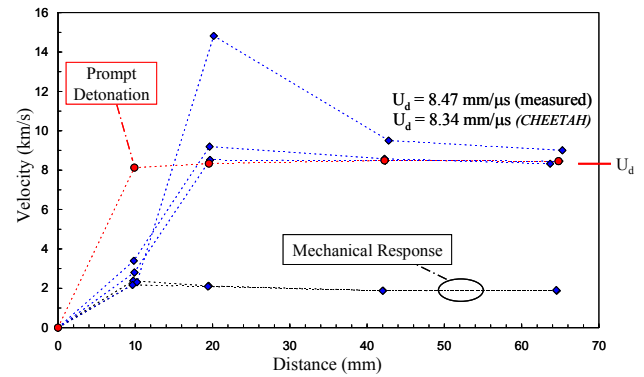


Fig. 4. Velocity calculations from PBXN-5 tests show non-shock initiation results, prompt detonation results, and CHEETAH predictions.

The non-shock insults that result in a mechanical response are observed to initially propagate above the PBXN-5 acoustic velocity (1.35 km/s), with a slight decrease in velocity as a function of distance.<sup>4</sup> The prompt-detonation control experiments show a velocity measurement that asymptotically approaches a steady velocity of 8.47 km/s, which shows that the CHEETAH calculations estimate of 8.34 km/s, is within 1.5% of the experimental velocity. The non-shock, or damage initiated experiments show the initial velocity to be above the detonation velocity followed by a rapid increase through the next 10-mm thick disc to approximately the detonation velocity. The observed transient overshoot in velocity is consistent with a Deflagration-to-Detonation Transition (DDT) in porous explosives, in which the porosity is caused by mechanical damage. This collection of experimental data at increasing impact velocities show that the non-shock initiation behavior, as shown in Figures 3 and 4, is dependent on input energy.

The average shock velocity through the assembled explosive billet is dependent on the specific energy input, as shown in Fig. 5 for each family of ideal explosives.

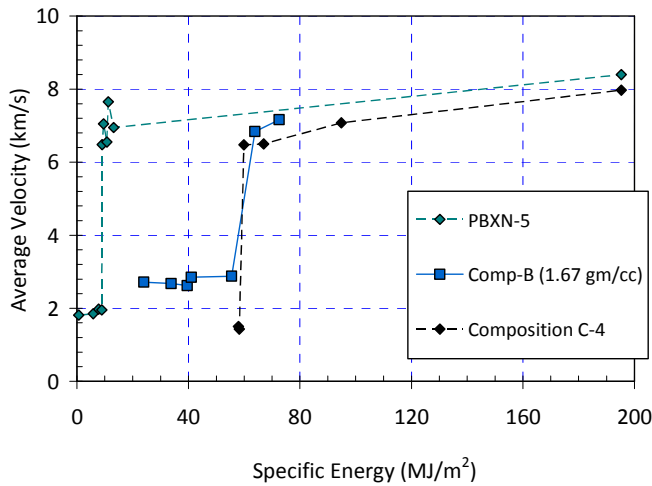


Fig. 5. Average velocity through explosive billet shows distinct transition to near-detonation velocity at initiation threshold, shown by family.

The average shock velocities range from slightly above acoustic velocity for mechanical response to nearly detonation velocity for a SDT-type reaction, with the velocity for non-shock initiations ranging between these limits. For energy inputs above the initiation threshold, the measured shock velocity is dependent on the run distance to the DDT transition. Baseline experiments used a M16 non-electric detonator for a SDT initiation, with a specific energy of 195.3 MJ/m<sup>2</sup>.

Experimental results are summarized for the rigid plastic bonded family in Table 1.

Table 1. PBXN-5 results, aluminum projectile.

Impact Velocity (m/s)	Impact Energy (kJ)	Specific Energy (MJ/m <sup>2</sup> )	Shock Velocity (km/s)
188	0.080	0.632	1.814
574	0.736	5.810	1.850
682	0.989	7.807	1.976
730	1.133	8.94	1.954
733	1.143	9.02	6.479
735	1.206	9.52	7.050
799	1.358	10.72	6.550
800	1.427	11.26	7.650
802 (tilt)	1.437	11.34	1.727
885	1.666	13.15	6.947
detonator	5.748	195.3	8.396

All damage initiation experiments were focused on specific energy levels below the SDT threshold. The PBXN-5 response to non-shock initiation showed a well defined initiation threshold of 9.0 MJ/m<sup>2</sup>, with modest scatter in the average velocity above the initiation threshold. The 802 m/s experiment had a 14-degree tilt angle on impact, resulting in a non-sustained deflagration with an average shock velocity of 1.727 km/s. The modest scatter in shock velocity above the initiation threshold is thought to be caused from lack of tilt control on the smooth-bore gas gun used for the PBXN-5 experiments. Subsequent testing on the cast, and moldable families used a rifled barrel powder gun to control tilt angle on impact.

The study of cast Comp-B used densities of 1.61, and 1.67 gm/cm<sup>3</sup>. The results from 1.61 gm/cm<sup>3</sup> cast Comp-B are given in Table 2.

Table 2. Cast Comp-B results, see projectile note.

Impact Velocity (m/s)	Impact Energy (kJ)	Specific Energy (MJ/m <sup>2</sup> )	Shock Velocity (km/s)
655 (B)	3.352	26.46	6.601
1,095 (A)	8.077	37.15	4.557
796 (B)	4.968	39.22	4.638
1,518 (A)	6.152	48.57	7.245
963 (B)	7.252	57.25	5.428
detonator	5.748	195.3	7.467

The projectile materials for the experiments shown in Table 2 were either aluminum (A) or brass (B) for the Comp-B experimental series, with the material notation following the impact velocity. The results from 1.67 gm/cm<sup>3</sup> cast Comp-B are given in Table 3.

Table 3. Cast Comp-B results.

Impact Velocity (m/s)	Impact Energy (kJ)	Specific Energy (MJ/m <sup>2</sup> )	Shock Velocity (km/s)
619	3.036	23.96	2.715
734	4.278	33.77	2.678
794	5.006	39.52	2.622
809	5.199	41.04	2.848
941	7.029	55.49	2.880
1010	8.089	63.86	6.841
1076	9.193	72.57	7.162

The cast Comp-B material showed an initiation threshold below 26.5 MJ/m<sup>2</sup> for the sample density of 1.61 gm/cm<sup>3</sup>, and an initiation threshold of 63.8 MJ/m<sup>2</sup> for a sample density of 1.67 gm/cm<sup>3</sup>.

The cast Comp-B initiation response shows a similar behavior to the rigid plastic bonded family for both densities when high quality material was studied. Experimental results from damaged Comp-B show an initiation threshold with a higher specific energy threshold than for the undamaged Comp-B, as shown in Fig 6.

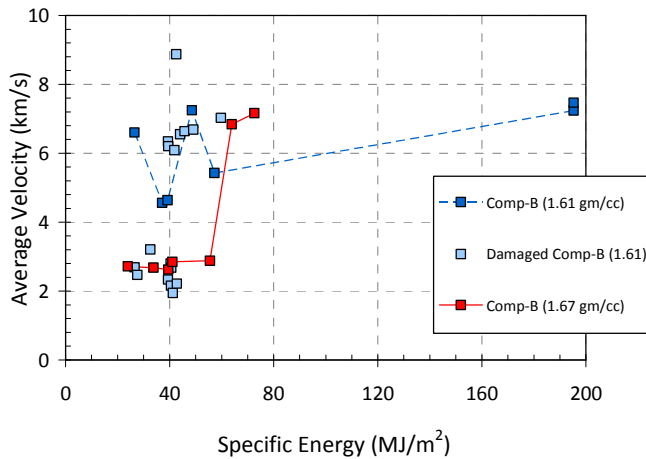


Fig 6. Density effects on Comp-B initiation threshold are observed, as well as the higher initiation threshold for damaged Comp-B.

The measurements on damaged Comp-B show considerable scatter in average velocity-vs-input energy for experiments near the initiation threshold. This scatter appears to be reasonable given that the material damage consists of cracks and voids with a length scale of several millimeters.

The moldable explosive family was investigated initially with a sandwiched billet configuration made with multiple layers of C2-thickness Primasheet 1000 (PETN), and 2000 (RDX) stacked and clamped together with the same arrangement of embedded PVDF shock sensors. Subsequent experiments with bulk moldable Composition C-4 used low density confinement rings to ensure a density of  $\rho=1.60$  gm/cc with known sample thicknesses. The results for the moldable family are shown in Fig. 7, and listed in Tables 4, 5, and 6.

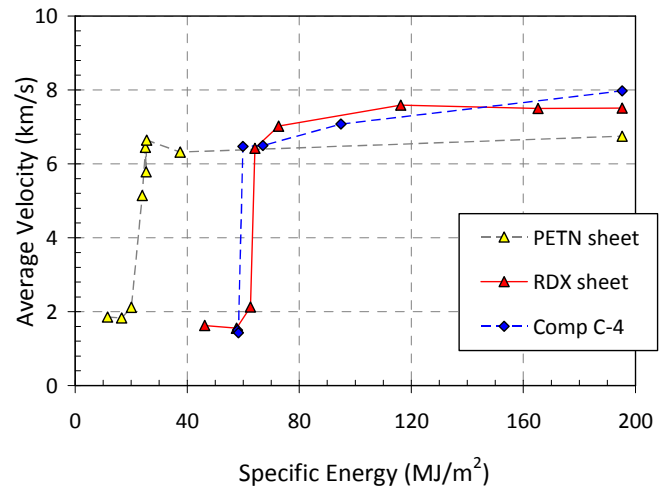


Fig. 7. Initiation thresholds for the moldable plastic explosive family, using both sheet and bulk material.

Table 4. Primasheet 1000 (PETN) results.

Impact Velocity (m/s)	Impact Energy (kJ)	Specific Energy (MJ/m <sup>2</sup> )	Shock Velocity (km/s)
432	1.463	11.55	1.859
517	2.100	16.58	1.829
569	2.541	20.06	2.119
622	3.032	23.94	5.145
637	3.178	25.09	6.443
640	3.208	25.32	5.785
642	3.231	25.51	6.643
778	4.746	37.47	6.321
detonator	5.748	195.3	6.748

Table 5. Primasheet 2000 (RDX) results.

Impact Velocity (m/s)	Impact Energy (kJ)	Specific Energy (MJ/m <sup>2</sup> )	Shock Velocity (km/s)
865	5.859	46.25	1.626
965	7.294	57.58	1.552
1006	7.927	62.58	2.130
1019	8.130	64.18	6.424
1083	9.201	72.63	7.021
1370	14.73	116.2	7.590
1634	20.93	165.2	7.497
detonator	5.748	195.3	7.506

Table 6. Composition C-4 results.

Impact Velocity (m/s)	Impact Energy (kJ)	Specific Energy (MJ/m <sup>2</sup> )	Shock Velocity (km/s)
968	7.339	57.93	1.502
971	7.383	58.29	1.429
985	7.589	59.91	6.475
1041	8.488	67.00	6.498
1238	12.02	94.88	7.078
detonator	5.748	195.3	7.973

The initiation response of the moldable explosive family demonstrates well defined thresholds for the two RDX-based materials, and a more gradual threshold for the PETN material. The RDX-based Primasheet 2000 exhibits no increase in average shock velocity above specific energy levels of 116 MJ/m<sup>2</sup>, with a lower detonation velocity than the Composition C-4.

### Thermal Effects

The initiation of explosives is known to be effected by initial temperature. The cast Comp-B material was chosen as the candidate material to evaluate the effect of temperature on non-shock initiation. Controlled experiments were conducted on Comp-B at elevated temperatures in the vicinity of the melt region, 63 – 122C using a thin walled, mild steel housing that was designed to retain the same configuration as the ambient temperature experiments, while housing molten Comp-B at the same density (1.67 gm/cm<sup>3</sup>). The effect of a mild steel housing was evaluated at ambient temperature in order to separate the effect of a steel housing from the effect of initial temperature. The results of those experiments are compared to ambient temperature tests, with and without a steel housing, as shown in Fig. 8.

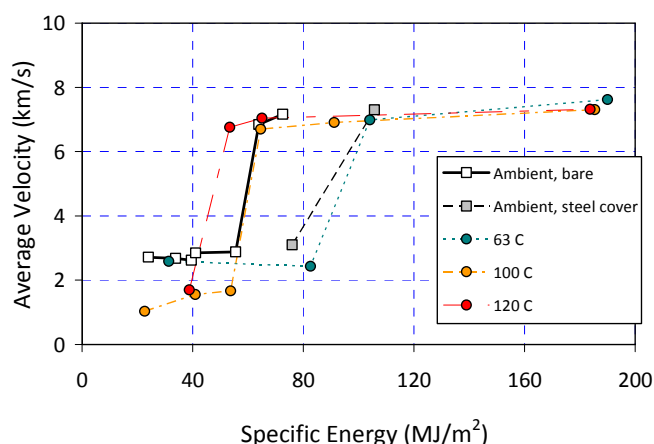


Fig 8. Thermal effect on initiation threshold of Comp-B.

The results of those elevated temperature experiments are listed in Tables 7, 8 and 9.

Table 7. Comp-B results at 63C.

Impact Velocity (m/s)	Impact Energy (kJ)	Specific Energy (MJ/m <sup>2</sup> )	Shock Velocity (km/s)
707	3.965	31.30	2.589
1148	10.47	82.64	2.433
1289	13.18	104.1	6.984
1627	24.07	190.0	7.622

Table 8. Comp-B results at 102C.

Impact Velocity (m/s)	Impact Energy (kJ)	Specific Energy (MJ/m <sup>2</sup> )	Shock Velocity (km/s)
601	2.866	22.63	1.033
808	5.186	40.94	1.554
926	6.806	53.73	1.667
1015	8.180	64.58	6.696
1206	11.55	91.18	6.904
1609	23.48	185.4	7.305

Table 8. Comp-B results at 122C.

Impact Velocity (m/s)	Impact Energy (kJ)	Specific Energy (MJ/m <sup>2</sup> )	Shock Velocity (km/s)
786	4.909	38.75	1.698
903	6.765	53.41	6.755
1019	8.239	65.04	7.041
1597	23.27	183.7	7.316

The effect of initial temperature on non-shock initiation behavior was evaluated both above and below the 85C melt temperature of Comp-B. The observations show that as initial temperature is increased from ambient, there is a slight increase in the specific energy initiation threshold at 63C, followed by progressive decrease in the initiation threshold as the initial temperature is increased above the melt to 122C. For specific energy levels below the initiation threshold, the average shock velocity was observed to decrease at temperatures above the melt. External piezoelectric shock sensors observed a transient overshoot in velocity near the initiation transition region, similar to the ambient temperature experiments.

### Summary

The initiation mechanism for ideal explosives subjected to impulsive loading from non-shock mechanical insults appears to be related to the input kinetic energy level and the material damage that is caused by shock and release wave interactions at the impact site that create additional surface area. For the experiments in the present study, the impulsive loading has sufficient time duration to compact this damaged material, initiating a DDT reaction, as evidenced by the transient super detonation velocities, which is observed for all explosive families at ambient temperature, and for Comp-B at elevated temperatures. The initiation thresholds are well defined for each explosive family. The cast Comp-B material with cracks and voids with a length scale of several millimeters appear to have a higher specific energy threshold for initiation, with more scatter than the undamaged Comp-B. The tests with RDX sheet material show that projectile impact at energy levels above 100 MJ/m<sup>2</sup> result in average velocities similar to the SDT initiation tests, even though the material experiences extensive damage from the shock loading and release profiles.

This study is directly coupled to the Damage-Initiated Reaction (DMGIR) model development, which has demonstrated the predictive capability to capture these effects.<sup>5</sup>

### Acknowledgements

The authors would like to thank Matthew Heine, Shawn Parks, Jason Podsednik, Don Gilbert and Shirley Smith at Sandia and Dennis Grady at Applied Research Associates for their contributions to this research program. Sandia is a multiprogram laboratory operated by Sandia Corporation, a Lockheed Martin Company, for the United States Department of Energy's National Nuclear Security Administration under Contract DE-AC04-94AL85000.

### References

1. Todd, S.N., "*Non-shock initiation model for plastic bonded explosive PBXN-5: empirical and theoretical results*", New Mexico Tech, PhD Dissertation, April 2007.
2. Anderson, M. U., et al, "*Prediction and data analysis of current pulses from impact-loaded piezoelectric polymers (PVDF)*", Shock Compression of Condensed Matter-1989, pp 805-808, 1990.
3. Anderson, M. U., et al, "*Non-Shock Initiation of the Plastic Bonded Explosive PBXN-5: Experimental Results*", Shock Compression of Condensed Matter-2007, pp 959-962, 2007.
4. Brown, G.W., *Dynamic and Quasi-static Measurements of PBXN-5 and Comp-B Explosives*, SEM 2009 Annual Conference and Exposition on Experimental and Applied Mechanics proceedings, June 2009.
5. Todd, S. N., et al, "*Non-Shock Initiation Model for Explosive Families: Numerical Results*", Shock Compression of Condensed Matter-2009, pp 361-364.